Root cortical senescence enhances drought tolerance in cotton

Liantao Liu[1], Congcong Guo[1], Ke Zhang[1], Hongchun Sun[1], Lingxiao Zhu[1], Yongjiang Zhang[1], Guiyan Wang[1], Anchang Li[1], Zhiying Bai[2], and Cundong Li[1]

[1]Hebei Agricultural University College of Agronomy
[2]Hebei Agricultural University

April 18, 2024

Abstract

The root cortex is an important anatomical phenes, and root cortical senescence (RCS) is closely associated with root absorptive function. However, characteristics and responses of RCS to drought stress in cotton have received little attention. This study subjected the drought-tolerant cotton variety "Guoxin 02" and the drought-sensitive variety "Ji 228" to drought stress (8% PEF6000) and no-stress (0% PEG6000) treatments to determine the characteristics and responses of cotton RCS to drought stress. The results showed that the RCS of the two varieties was significantly promoted under drought stress. The greater the distance from the root tip, the more severe the RCS occurrence under drought stress compared with non-stress treatment. The occurrence of RCS in "Guoxin 02" highered by 14.03%-20.18% compared to "Ji 228" under drought stress. Moreover, the RCS was significantly negatively correlated with root respiration but significantly positively correlated with total root length and leaf water potential ($p < 0.05$). Indole-3-acetic acid (IAA) content increased, while abscisic acid (ABA) content decreased as the RCS increased. In summary, endogenous hormones regulated the occurrence of RCS, which reduced the root metabolic costs and seemingly achieved more resource redistribution to new roots, thereby expanding the water absorption capacity of roots to fully utilize deep water resources. Thus, the study demonstrates the potential of RCS in improving the drought stress tolerance of cotton.

Root corticalsenescenceenhancesdrought tolerance in cotton

Congcong Guo[1], Ke Zhang[1], Hongchun Sun[1], Lingxiao Zhu[1], Yongjiang Zhang[1], Guiyan Wang[1], Anchang Li[1], Zhiying Bai[2*], Liantao Liu [1*], Cundong Li[1*]

[1] State Key Laboratory of North China Crop Improvement and Regulation/ Key Laboratory of Crop Growth Regulation of Hebei Province/ College of Agronomy, Hebei Agricultural University, Baoding, Hebei 071001, China

[2] State Key Laboratory of North China Crop Improvement and Regulation, College of Life Science, Hebei Agricultural University, Baoding 071000, China

* Correspondence:

Liantao Liu, *liultday@126.com*

Cundong Li, *auhlcd@163.com*

Zhiying Bai, *zhiyingbai@126.com*

Abstract

The root cortex is an important anatomical phenes, and root cortical senescence (RCS) is closely associated with root absorptive function. However, characteristics and responses of RCS to drought stress in cotton have received little attention. This study subjected the drought-tolerant cotton variety "Guoxin 02" and the

drought-sensitive variety "Ji 228" to drought stress (8% PEF6000) and no-stress (0% PEG6000) treatments to determine the characteristics and responses of cotton RCS to drought stress. The results showed that the RCS of the two varieties was significantly promoted under drought stress. The greater the distance from the root tip, the more severe the RCS occurrence under drought stress compared with non-stress treatment. The occurrence of RCS in "Guoxin 02" highered by 14.03%-20.18% compared to "Ji 228" under drought stress. Moreover, the RCS was significantly negatively correlated with root respiration but significantly positively correlated with total root length and leaf water potential ($p < 0.05$). Indole-3-acetic acid (IAA) content increased, while abscisic acid (ABA) content decreased as the RCS increased. In summary, endogenous hormones regulated the occurrence of RCS, which reduced the root metabolic costs and seemingly achieved more resource redistribution to new roots, thereby expanding the water absorption capacity of roots to fully utilize deep water resources. Thus, the study demonstrates the potential of RCS in improving the drought stress tolerance of cotton.

KEYWORDS: Root cortical senescence, Cotton, Drought tolerant, Root metabolic costs

1 Introduction

Root anatomical phenes play a pivotal role in capturing soil resources, and the root cortex is a vital anatomical phene found between the epidermis and stele. The root cortex consists of multiple layers of thin-walled cells differentiating from the primary meristem, occupying a significant proportion of the root cross-section volume. The cortex is a lateral pathway for water and solute transport from root hairs to the central cylinder, serving as the primary site for nutrient storage, aeration, and secretion of nutrients and growth regulators (Lynch, 2015). Root cortical senescence (RCS) is a form of programmed cell death occurring in the cortical cells of the root system (Schneider and Lynch, 2018). During RCS, the root external appearance remains healthy and white, but the cortical cells predominantly lose their nuclei (Bingham, 2007), a phenomenon commonly referred to as "non-pathogenic root cortex death" (Deacon and Henry, 1978).

Accurately quantifying RCS is essential for comprehensively understanding plant growth and physiological status. Histological techniques utilizing cell viability staining have become the predominant approach for studying RCS phenotypes. Commonly used dyes, including neutral red (Beckel, 1956), Feulgen reagent (Holden, 1975), toluidine blue (Brown and Hornby, 1987), acridine orange (Henry and Deacon, 1981), and other cell viability stains, have demonstrated efficacy in RCS assessment. While concerns were raised by Wenzel and McCully (1991) about the effectiveness of acridine orange and other cell viability staining dyes for RCS evaluation, research by Henry and Deacon (1981) indicated a higher potency in RCS detection when assessed using acridine orange staining, Feulgen staining, and single-cell pressure probe techniques (Bingham, 2007). Similar to acridine orange staining, technologies such as single-cell turgor pressure measurements, TUNEL-assay and Nomarski optics revealed comparable RCS patterns and occurrence rates across various plant species (Bingham, 2007; Henry and Deacon, 1981; Liljeroth and Bryngelsson, 2001; Wenzel and McCully, 1991). These research findings confirm the feasibility of using acridine orange and other cell viability staining methods to evaluate RCS.

RCS causes the damage or loss of nuclei in the cortical cells, an early indicator of cell apoptosis and RCS manifestation. Therefore, anucleated cortical cells are the hallmark of RCS, and the number of viable cells gradually diminishes with increasing cortical aging (Liljeroth, 1995). RCS significantly impacts the morphology and physiological characteristics of the root system; for example, during RCS, the cross-sectional area of the root cortex decreases, restricting the radial transport pathways from the cortex to the stele (Liljeroth, 1995). The occurrence of RCS also increases the proportion of aerenchyma in the root cortex of Gramineae crops, thus inhibiting the cortex function and increasing nutrient and water transport resistance (Hu et al., 2014a; Schneider et al., 2017b; Galindo-Castañeda et al., 2018). RCS has been shown to decrease the metabolic consumption of photosynthetic products in the cortex, especially during drought stress, with a substantial portion being utilized for new root growth (Lynch, 2015). This, in turn, promotes root elongation (Chimungu et al., 2015; Schneider et al., 2017b) and enhances water uptake (Lynch et al., 2005). Thus, it is evident that RCS is closely associated with the functionality of the root system under adverse conditions.

The RCS occurrence is influenced by multiple factors., including crop variety, growth stage, culture medium type, position within the root system, stress conditions, and phytohormones (Liljeroth, 1995; Schneider et al., 2017b). For instance, wheat seedling roots exhibited the highest rate of RCS occurrence compared to rye, barley, and oats (Henry and Deacon, 1981). Stress conditions such as low nitrogen, low phosphorus, and drought also induce the occurrence of RCS (Liljeroth, 1995). Compared with the root segments without RCS, the ones with RCS decreased by 19% and 12% under high N and low N conditions, respectively (Schneider et al., 2017b). The occurrence rate of RCS is also regulated by ethylene (Schneider et al., 2018), and exogenous ethylene significantly increases the RCS occurrence in maize seedlings and lateral roots (Schneider et al., 2018). However, the characteristics of RCS occurrence and its response to drought stress in Malvidae cotton are rarely reported.

Drought stress significantly constrains global agricultural productivity (Lynch, 2007), and efficient acquisition of soil moisture is crucial for enhancing plant drought tolerance. Cotton (*Gossypium hirsutum* L.) is a valuable economic crop. As a straight-rooted crop, cotton exhibits a well-developed root system with a deep tap root and widely distributed lateral roots. The function level and physiological metabolism of the root cortex largely represent the functionality and metabolism of the entire root system. Previous studies on gramineous crops found that unfavorable conditions accelerated RCS, reduced root respiration and decreased the transfer and allocation of photosynthetic products to fast-growing tissues (Schneider et al., 2017b). The anatomical structures of the root systems of dicotyledonous and monocots differ; however, the response mechanisms of RCS to stress conditions have not been reported in dicotyledonous crops. Therefore, there is a need to investigate the RCS responses of dicotyledonous crops to stress conditions. There are several unresolved questions regarding the effects of RCS in cotton: Is the susceptibility of the aboveground parts of cotton to drought due to premature RCS? What are the spatio-temporal variation characteristics and patterns of RCS in cotton? Is there a correlation between the consumption of a substantial quantity of photosynthates by RCS and the resilience of the aboveground parts of cotton?

We hypothesize that endogenous hormones regulate RCS in drought-tolerant varieties under drought stress, leading to reduced root metabolic costs. Consequently, more energy is redirected towards root growth, thereby enhancing drought tolerance. Therefore, this study aimed to explore the causative factors of cotton RCS and its physiological metabolism and endogenous hormonal regulation under drought stress, clarify the physiological role of RCS occurrence in relation to the regulation of the whole root development, and reveal the physiological mechanism of RCS in relation to the drought tolerance of cotton aboveground parts. The study mainly focused on (1) evaluating the existence and occurrence patterns of RCS in cotton and assessing the characteristics of cotton RSC under drought stress; (2) clarifying the characteristics and patterns of metabolic activities and endogenous hormones and their interrelationships during the RCS in cotton; (3) exploring the mechanism of action and effects of RCS on the root system and aboveground parts of cotton. This study is the first to confirm the existence of RCS in a dicotyledonous crop, cotton, and provides an in-depth understanding of the characteristics and patterns of RCS under drought stress. The results form the basis for using RCS to improve drought tolerance in cotton.

2 Materials and Methods

2.1 Experimental design

The experiment was conducted in the greenhouse at Hebei Agricultural University (38°85'N, 115°30'E) in Baoding Hebei Province, China. Two cotton varieties, the drought-tolerant type "Guoxin 02" (DT type) and the drought-sensitive type "Ji 228" (DS type), were selected for this study (Guo et al., 2022). After sterilization with 75% ethanol, the seeds were rinsed 5-8 times repeatedly with distilled water, then soaked in distilled water for 8 hours and placed on a towel to germinate. The radicle was transferred to a hydroponic pot at 2 cm. Once the cotyledons were fully expanded, the samples were transferred to an incubator (485*355*245 mm) for continued hydroponic growth in the Hoagland nutrient solution. Each incubator contained 24 seedlings and 50 L of Hoagland's nutrient solution.

Cotton plants were grown to the two true leaf stages, at which point water treatments were initiated. The

treatments included no-stress (NS, 0% PEG6000) and drought stress (DS, 8% PEG6000) for 15 days, and each treatment had 24 replications. The pH of the nutrient solution was adjusted to 6.0 ± 0.1, and the solution was replaced every 3 days. The growth parameters included an average daily temperature of approximately (28 ± 2) / (25 ± 2) °C (day/night), a photoperiod of 14/10 hours of light/darkness, relative humidity of 40%-50%, and a light intensity of 600 μM. Oxygen was supplied twice daily, with each session lasting 30 minutes.

2.2 Acridine orange staining and anatomical characterization

Root segments (approximately 0.5 cm) were sampled in triplicate at 3 cm, 6 cm, 9 cm, and 12 cm from the taproot root tip 15 days after the drought stress treatment. The root segments were stored in 75% ethanol and phenotypically analyzed for the presence of RCS in the cortex using acridine orange staining, as described by Henry and Deacon (1981). Acridine orange staining is a viable method to assess RCS. Acridine orange fluorescent nuclei were used for phenotyping the onset of RCS within individual cortical layers. The disappearance of the cortex, determined by the percentage of viable cells, was used to indicate RCS manifestation at the root cross-sectional level. The acridine orange-stained root segments were embedded in a gelatin capsule with Tissue-Tek CRYO-OCT compound (Thermo Fisher Scientific, Waltham, MA, USA) and snap-frozen in liquid nitrogen before storage at -20 °C. Cross-sections (8 μm thick) of the embedded segments were cut using a Freeze Slicer (Leica CM1950) and imaged using a laser scanning confocal microscope (FV-1000, Olympus, Japan).

The main measurements using the cross-sectional images included area determination and variable counting. The following area measurements were obtained through pixel counting: the total cross-section area and diameter, the stele area and diameter, and the cortex area and diameter. The average cell size was also calculated by pixel counting, and the cortical areas of acridine orange fluorescent nuclei were measured. The number of acridine orange fluorescent nuclei was counted in all cell layers of the 8 μm thick sections. The count data included the number of cortical cells, cortical cell files, and cortical lacunae area. The calculation formulas were as follows (Schneider et al., 2017b; Schneider et al., 2017a; Schneider et al., 2018; Schneider and Lynch, 2018):

Cortical area = Cross section area Stele area(1)Cortical diameter = Cross section diameter Stele diameter(2)Stele/whole r
(3)Lacunae/cortex ratio = Total lacunae area/Cortex area (4)Cortex/stele ratio = Cross section area/Stele area
(5)

RCS-free control samples were root segments collected at 3 cm from the root tip (Schneider et al., 2017b). The cortical senescence percentage was calculated by comparing the cortical area (total cross-sectional area - stele area) at 3 cm from the root tip with the corresponding area on the sampled position (Schneider et al., 2017b).

2.3 The root metabolic enzyme activity and root respiration

Root segments (approximately 0.5 cm) sampled at 3 cm, 6 cm, 9 cm, and 12 cm from the taproot root tip 15 days after drought stress treatment were used to measure root metabolic enzyme activity and root respiration. The measurements were conducted in triplicate.

Phosphofructokinase activity levels were determined using the method described by Baldwin et al. (2007), and changes in absorbance were monitored continuously at 340 nm.

Malate dehydrogenase activity levels were determined using the method described by Childress and Somero (1979), whereby the NADH oxidation was quantified at 340 nm. Glucose-6-phosphate dehydrogenase activity induced by the reduction of NADP+ to NADPH was measured at 340 nm (Antonietta Ciardiello et al., 1995).

Root respiration was measured for 10 minutes using a LI-840A CO_2/H_2O gas analyzer (LI-COR, Inc., Lincoln, NE, USA), after which the root segment was dried and weighed (Sun et al., 2021).

2.4 Endogenous hormone content

Root segments were sampled as described in section 2.3. Phytohormone, gibberellin (GA), zeatin riboside (ZR), indole-3-acetic acid (IAA), brassinolide (BR) and abscisic acid (ABA) contents in the root segments were determined using an Agilent 1260 High-Performance Liquid Chromatograph with an Eclipse XDB-C18 column (250 mm × 4.6 mm, 5 mm, Agilent, CA, United States).

Briefly, 2 g of fresh root segments were ground in 10 mL of pre-cooled 80% methanol in an ice bath. After centrifugation at 8,000 g for 10 minutes at 4°C, the supernatant was collected, and the residue was resuspended in 8 mL pre-cooled 80% methanol, followed by another round of centrifugation and supernatant collection. The aqueous phase was then extracted three times with 20 mL of ethyl acetate. The sample was evaporated and dried at 40°C under pressure, and the separation of the five endogenous phytohormones was conducted via gradient elution (Zhang et al., 2013).

2.5 Root system phenotyping

Root samples were obtained in triplicate at 0, 5, 10, and 15 days after drought stress treatment. Digital images with a resolution of 600 dots per inch were obtained using a scanner (EPSON Expression 10000XL). The root images were analyzed using WinRHIZO (Regent Instruments, Inc., Quebec City, Canada) and RootNav software (Christopher et al., 2013; Pound et al., 2013) to obtain information on the root traits (Table S1) (Zhang et al., 2021).

Thereafter, the fresh weight of the roots and aboveground parts was obtained by weighing, and the biomass was obtained by drying at 105 °C for 30 minutes and then at 75 °C for 72 hours to constant weight.

2.6 Morphological and physiological traitsof the aboveground parts

Aboveground parts were sampled as described in section 2.5. Plant height was measured using a straightedge, and leaf area was calculated using the length and width factor method. Stem diameter was recorded with a vernier caliper.

The ratio of variable to maximum fluorescence (F v/F m) was measured using a portable Chlorophyll Fluorescence monitoring system (FMS-2, Hansatech, King's Lynn, UK). The relative chlorophyll content was measured using a SPAD chlorophyll meter (SPAD-502; Konica Minolta, Tokyo, Japan) while avoiding the leaf veins. The leaf water potential was measured with a Model 600 plant pressure chamber (PMS, USA), while stomatal size and density were measured using a combination of nail polish and sticky tape. The relative water content and leaf water saturation deficit were determined by weighing (Yang et al., 2022). These measurements were based on the third functional leaf and were conducted between 9:00 and 11:00.

2.7 Statistical analysis

Microsoft Excel 2019 (Statistical Product and Service Solutions) was used to record and organize the data. Analysis of variance (ANOVA) was performed using SPSS 26.0 (IBM Corp., Armonk, NY, USA), and graphs were generated using Origin 2019b and GraphPad Prism 9.0 (GraphPad Software, Inc., San Diego, CA, USA). Schematics and typography were created using Adobe Illustrator 2020, and structural equation modeling was conducted using R version 4.3.1. Phenotypic analysis of the root cross-sectional images was performed using Image J software.

3 RESULTS

3.1 Cortical senescence percentage, cortical cell files and cortical lacunae area indicate the progress of RCS

To investigate the spatio-temporal characteristics of cotton RCS, we employed a laser scanning confocal microscope to scrutinize the anatomical structures from the root tip to the root end, as depicted in Figure 1. The lacunae area is the principal indicator of RCS. Drought stress significantly promted the degree of lacunae area. In other words, the lacunae area was larger in tissues far from the root tip under drought stress compared to no-stress treatment. Both varieties exhibited an increasing lacunae area with the increasing

distance from the root tip under no-stress conditions (Figure 1). The occurrence of RCS varied in the two varieties. Under drought stress, RCS in "Guoxin 02" significantly increased compared to "Ji 228.".

The cortical senescence percentage, cortical cell files and cortical lacunae area provide the basis for evaluating the progression and patterns of RCS within the root sections (Schneider et al., 2017b). The percentage of the senescent cortex is used to compute the disparity in cross-sectional areas (total cross-sectional area — stele area) at 3 cm from the root apex and at the sample position (Schneider et al., 2017b). Essentially, this determines the difference in the cross-sectional area between the sample and the root tip, providing a quantitative measure of cortical senescence. Among these parameters, cortical senescence percentage is a key indicator for evaluating RCS. RCS was evidenced by the disappearance and absence of the root cortex, which included cortical cell files and cortical lacunae area (Figures 2BC).

Drought stress significantly promoted the occurrence of RCS in cotton. Compared with no-stress, the cortical senescence percentage in "Guoxin 02" increased significantly by 26.26%-56.69% (Range of all root segments) and by 22.56%-35.48% in "Ji 228" under drought stress (Figure 2A).

Changes of the cortical senescence percentage in different root segments. Under drought stress, the occurrence of RCS was directly proportional to the distance from the root tip, meaning that the frequency of RCS significantly increased with increasing distance from the root tip (Figure 1). The cortical senescence percentage of "Guoxin 02" and "Ji 228" at 12 cm segment from the root tip was 82.43% and 75.64% higher than that at the 6 cm root segment, respectively (Figure 2A).

Significant genotypic differences in RCS were also observed between "Guoxin 02" and "Ji 228" ($p < 0.01$). After 15 days of drought stress, "Guoxin 02" had a higher occurrence rate of RCS than "Ji 228". Specifically, the cortical senescence percentage of the "Guoxin 02" increased significantly from 14.03% to 20.18% compared to "Ji 228" under drought stress. (Figure 2A).

Drought stress significantly reduced the cortical cell files (Figure 2B) of cotton but significantly increased the cortical lacunae areas (Figure 2C). Specifically, compared with no-stress treatment, the cortical lacunae area of "Guoxin 02" and "Ji 228" significantly increased by 9.45 - 32.65 and 0.51 - 1.79 times, respectively, under drought stress (Figure 2C). The cortical lacunae area significantly increased with increasing distance from the root tip. Specifically, the cortical lacunae area of "Guoxin 02" and "Ji 228" increased significantly by 26.13 times and 4.82 times, respectively, in the 12 cm segment compared to the 3 cm segment from the root tip (Figure 2C).

3.2 Association between RCS and reduced root metabolic costs

Schneider et al.(2017b) established a negative correlation between RCS and root metabolic costs. Therefore, to further underscore the occurrence of RCS in cotton crops, we conducted a comprehensive series of experiments involving measuring the changes in root metabolic enzyme activities and root respiration across different root segments (Figure 3).

Compared to no-stress, drought stress reduced the phosphofructokinase, malate dehydrogenase, and glucose-6-phosphate dehydrogenase activities, and root respiration by 0% - 21%, 32% - 34%, 46% - 51%, and 20% - 63% in "Guoxin 02" and by 5% - 19%, 31% - 39%, 23% - 37%, and 9% - 34% in "Ji 228", respectively (Figures 3A-D).

Notably, the trend characteristics at different locations from the root tip to the root end showed that RCS was inversely proportional to phosphofructokinase, malate dehydrogenase, and glucose-6-phosphate dehydrogenase activities, and root respiration. That is, phosphofructokinase, malate dehydrogenase, and glucose-6-phosphate dehydrogenase activities, and root respiration decreased significantly with increasing distance of the root segments from the root tips (Figures 3A-D). Specifically, compared to the 3 cm root segments, phosphofructokinase, malate dehydrogenase, and glucose-6-phosphate dehydrogenase activities, and root respiration significantly decreased by 15.28%, 10.34%, 12.76%, and 71.56% in "Guoxin 02", (Figures 3B-D) and by 32.96, 25%, 34.46%, and 57.66% in "Ji 228", respectively (Figures 3A-D), in the 12 cm root segments under drought stress.

In addition, root metabolic costs varied significantly among varieties. Compared with "Ji 228", root respiration and glucose-6-phosphate dehydrogenase activity of "Guoxin 02" decreased by 26.78% and 19.39% (whole root segment), respectively, under drought stress (Figures 3DC). Pearson correlation analysis showed that the cortical senescence percentage at 6 cm, 9 cm and 12 cm from the root tip was positively correlated with root respiration (p <0.05, Figures 4D-F). In summary, the trends we observed in root metabolic costs provide further scientific evidence of the presence of RCS in cotton.

3.3 RCS affects thetissue structure of the root cortex

The characteristics of each tissue structure in the different root segments during RCS development were further analyzed (Figure 5A). Drought stress increased the stole/whole ratio (Figure 5B) and lacunae/cortex ratio (Figure 5C) but reduced the cortex/stele ratio (Figure 5D).

Notably, the trend characteristics at different locations from the root tip to the root end showed that RCS was directly proportional to the stele/whole ratio, lacunae/cortex ratio, cross-section area, cross-section diameter, stele area, stele diameter, cortical area, and cortical diameter, but inversely proportional to the cortex/stele ratio. That is, the stele/whole and lacunae/cortex ratio increased significantly (Figures 5HJ), but the cortex/stele ratio decreased significantly with increasing RCS (Figure 5I). Specifically, the stele/whole ratio and the lacunae/cortex ratio increased by 7.14% - 60.60% and 50% - 133.33%, respectively, at the 12 cm segments compared to 3 cm segment from the root tip (Figures 5HJ).

There were genotypic differences in the proportion variation of each tissue structure. Among them, the stele/whole and lacunae/cortex ratios of "Guoxin 02" were significantly higher (94.22% and 117.02%, respectively) than those of "Ji 228" under drought stress (Figures 5HJ). However, the cortex/stele ratio was significantly reduced (58.97%) (Figure 5I).

3.4 RCSis inversely proportional to endogenous hormones

To characterize the changes in endogenous hormone levels during RCS development in cotton and the mechanism of their influence, we measured the contents of five endogenous hormones in different root segments. GA, ZR, IAA, and BR contents were decreased under drought stress compared to the no-stress treatment (Figures 6A-D); however, ABA was increased (Figure 6E).

Notably, the trend characteristics at different locations from the root tip to the root end showed that RCS was inversely proportional to GA, ZR, IAA, BR, and ABA contents. That is, GA, ZR, IAA, BR, and ABA decreased significantly with increasing distance from the root tips (Figures 6A-E). Specifically, compared to 3 cm root segments, GA, ZR, IAA, BR, and ABA contents of "Guoxin 02" significantly decreased by 28.93%, 68.91%, 35.82%, 65.15%, and 60.01%, respectively, in the 12 cm root segments under drought stress (Figures 6B-D). Similarly, the GA, ZR, IAA, BR, and ABA contents of "Ji 228" significantly decreased by 47.12%, 60.97%, 56.14%, 69.10%, and 40.25% in the 12 cm root segments compared to the 3 cm root segments, respectively, under drought stress (Figures 6B-D). The endogenous hormonal content of each segment differed between the two varieties. Compared with "Ji 228", the GA and ABA contents of "Guoxin 02" decreased by 24.74% - 44.46% (Figure 6A) 31.28% - 54.01% (Figure 6E), respectively, but IAA increased by 10.93% - 69.33% (Figure 6C).

Linear regression analysis showed a significant correlation between RCS and the endogenous hormone content of the root system. GA and ABA contents showed a decreasing trend with the increasing cortical senescence percentage at 6 cm, 9 cm and 12 cm segments from the root tip under drought stress (Figures S1 A-C and G-I). However, IAA showed an increasing trend (Figures S1 D-F). Notably, the cortical senescence percentage at the 12 cm segment from the root tip significantly correlated with GA, ABA, and IAA contents ($0.01 < p < 0.05$).

3.5 RCS is closely related to root and aboveground growth

To clarify the physiological role of RCS in regulating the development of the whole root system and aboveground parts, we measured several traits, such as root architecture and shoots, at different time points

(Figures 7-8). There were genotypic differences in the response of cotton roots to drought stress (Figure 7A). Specifically, compared to "Ji 228", the total root length, root dry weight, specific root surface area, root volume, root tissue density, average length - lateral roots, average length - all roots, and convex hull area of the "Guoxin 02" were increased by 45.92%, 90.00%, 98.70%, 37.56%, 84.00%, 28.04%, 30.63%, 16.97%, and 15.65%, respectively, under drought stress (Figures 7BCDEGIJM). However, the lateral root angle was significantly reduced by 23.34% (Figure 7K).

The impact of drought stress on aboveground traits of cotton plants was the highest at 15 days after treatment (Figure S2 and Figure S3). Under drought stress, the F v/F m, leaf area, leaf water potential, plant height, relative leaf water content, stomatal length, stomatal width, and stomatal opening of "Guoxin 02" increased by 80.21%, 40.05%, 15.56%, 18.42 %, 29.91%, 15.09%, 23.68%, and 18.75%, respectively, (Figures 8ABCFGIJK) compared to "Ji 228". However, the leaf water saturation deficit and stomatal density showed a significant reduction of 9.79% and 5.91%, respectively (Figures 8EL).

Pearson correlation analysis showed that the cortical senescence percentage at the 6 cm, 9 cm and 12 cm segments from the root tip were positively correlated with root total length, root dry weight, root tissue density, leaf water potential, leaf relative water content, and$F$ v/F m ($p < 0.05$, Figures 3ABCGHI).

3.6 Structural equation model of RCS and drought tolerance

To further investigate the direct and indirect effects of RCS on cotton drought tolerance, we generated a structural equation model to examine the relationship between RCS and cotton drought tolerance and determine the path coefficients between the two (Figure 9). The structural equation model showed a significant correlation between RCS and drought tolerance, with a P -value of 0.033*. This indicated that the pathway was valid, with an effect coefficient of 0.986. Overall, the model demonstrated a good fit (Table S2).

4 Discussion

4.1 Characteristics and patterns of RSC in cotton under drought stress

This study reports for the first time the presence of the RCS in cotton, a dicotyledonous crop of the mallow family. RCS has been widely explored in monocotyledons, including wheat, triticale (*Triticosecale*), barley (Yeates and Parker, 1986; Liljeroth, 1995), rye (*Secale cereale*) (Deacon and Mitchell, 1985; Jupp and Newman, 1987), and oats (*Avena sativa*) (Yeates and Parker, 1986). However, there are no reports of RCS in dicotyledonous crops. The study also explored the characteristics and occurrence mechanism of RSC in cotton under drought stress.

To determine the spatio-temporal variation in the occurrence of RCS in cotton, we examined the cortex to determine the absence of acridine orange-stained fluorescent nuclei (Henry and Deacon, 1981). The two cotton varieties showed a similar pattern of RCS, which started in the outer cortical cell region and progressed inward. RCS was triggered mainly by non-apoptotic programmed cell death of cortical cells involving cells between the inner and outer cortex. According to laser scanning confocal microscopy, the gap between the cortical cells increased, and the cortical cells aged and underwent autolysis, with their internal structures gradually disintegrating with the occurrence of RCS. This disintegration gradually led to cortical cell contraction and invagination. When the internal material was depleted, the residual cell walls of the adjacent cells were superimposed, forming air spaces on both sides. Despite the senescence and disintegration of the cortex, the outer epidermis remained intact, and the outer epidermis, the air space, and the stele were clearly distinguishable (Figure 1). Different parts of the cotton root system, from the root tip to the root end, reflect the root developmental processes, including root cell genesis, differentiation, maturation, and death. In the root cross-section of cotton grown under no-stress conditions, the root tip zone (3 cm from the root tip) was almost devoid of RCS, but the root basal zone (12 cm from the root tip) showed partial RCS. In summary, the spatial dimension reveals that RCS shows an increasing trend in cotton with the increasing distance from the root tip; that is, root cortical cells exhibit dynamic changes from nucleated to non-nucleated forms from about the 3 cm region of the root tip to the junction of the taproot (Figure 1).

Analysis of the acridine orange fluorescent nuclei in the cortical area, cortical cell files, and cortical lacunae

area also highlighted significant changes in different locations from the root tip to the root end. The cortical lacunae area showed a gradual increase (Figure 2C), while cortical cell files showed an initial increase followed by a decrease (Figure 2B), indicating that RCS mainly occurred in the maturation zone. Notably, the stele remained viable despite the occurrence of RCS, as demonstrated by the acridine orange fluorescent nuclei. The proportion of the root tissues also changed dynamically with increasing distance from the root tips (Figure 5). For example, the stele/whole ratio and lacunae/cortex ratio increased (Figure 5BD), while the cortex/stele ratio decreased (Figure 5C) with increasing root tip distance.

Drought stress induced RCS in cotton. The root profile of cotton grown under drought stress showed different spatio-temporal variations: the root tip zone (3 cm from the root tip) was almost devoid of RCS, while the root middle zone (6 cm from the root tip) showed partial RCS, and the root end zone (12 cm from the root tip) showed the highest RCS rate. However, drought stress did not change the occurrence point of RCS relative to the root tip, but it did increase the degree of RCS occurrence in cotton. After 15 days of drought stress treatment, the cortical cells of cotton roots showed senescence, leaving only root tips (Figure 1). Unlike the no-stress condition, the greater the distance from the root tip, the more severe the RSC degree under drought stress, which seriously affects root function. Therefore, we suggest that the cotton aboveground resilience may exhibit reduced drought tolerance due to premature RCS. Moreover, a previous study demonstrated that under low P and low N conditions, the RCS of barley increased by 13% and 11%, respectively (Schneider et al., 2017b), while shading decreased the RCS of wheat and barley (Lewis and Deacon, 1982). Thus, RCS is a complex phenomenon that depends on environmental factors, plant species, and genetic factors (Liljeroth, 1995; Schneider et al., 2017a).

The extent to which RCS occurs varies among plant species. For example, in 15-day-old wheat roots, 80% - 90% of the root cortical cells were non-nucleated (Liljeroth, 1995), whereas only 20% - 35% were non-nucleated in barley and rye (Liljeroth, 1995). This suggests that wheat has a relatively higher degree of RCS compared to other plants (such as wheat, barley, rye, and oats) (Deacon and Henry, 1980; Deacon and Mitchell, 1985; Henry and Deacon, 1981; Holden, 1976; Liljeroth, 1995; Yeates and Parker, 1986). However, the comparison of RCS between cotton and other crops has not been reported. Our study showed that only 40% - 50% of the root cortical cells of cotton plants grown for 31 days (from planting to harvesting) were non-nucleated (Figure 2B). Thus, the degree of RCS in the 31-day-old cotton roots was reduced by about 20% compared to the 15-day-old wheat. Therefore, the incidence of RCS in cotton was lower than in wheat; however, this should also be compared with other crops (such as triticale, barley, rye, and oats).

RCS exhibits significant genetic variability in cotton. The two cotton varieties (with different drought tolerance) used in this study showed significant differences in RCS. "Guoxin 02" had a significantly higher rate of RSC than "Ji 228" under drought stress (Figure 2A), indicating that a higher RCS rate may be a key feature of the plant's ability to cope with drought stress. Similarly, differences in RCS have been reported between wheat and barley varieties (Henry and Deacon, 1981; Liljeroth, 1995). Therefore, the variation in RCS was mainly influenced by the genotypic differences under drought stress. However, the genetic and molecular mechanisms underlying this variation in cotton need further exploration.

4.2 RCS reduces root respiration

Root respiration is closely related to root maintenance costs. Root respiration, growth, maintenance, and ion uptake are the main components of root metabolic costs (Lambers, 1979; Van Der Werf et al., 1988; Lynch et al., 2005). Root metabolic costs involve changes in the internal configuration of the organelle, where the thickness between the cytoplasm and the vacuole membrane remains constant, such that the increase in RCS is mainly due to increased vacuole size (Gunawardena et al., 2001). Increased vacuole volume relative to the cytoplasm may reduce respiration because metabolic activity is higher in the cytoplasm than in the vacuole (Schussler and Longstreth, 1996). Our study quantified cotton root respiration in the mature region and found that total respiration in this region primarily involves tissue maintenance respiration. By inducing the transition from nucleated to non-nucleated cells, RCS alters the maintenance of respiration in the mature zone, emphasizing the need to maintain metabolic homeostasis in the cotton root system (Lynch et al., 2005; Lynch and Brown, 2008). Since RCS mainly occurs in the mature zone of the cortex, it affects root

maintenance costs rather than construction costs. Therefore, we hypothesized that under drought stress, RCS significantly affects maintenance costs rather than construction costs and greatly impacts the ability of plants to adapt to arid environments.

This study revealed, for the first time, a significant negative correlation between RCS and root respiration in cotton under drought stress ($p < 0.01$, Lynch, 2015). Compared with "Ji 228", the root respiration and glucose-6-phosphate dehydrogenase activity (whole-root segment) of drought-resistant variety decreased by 26.78% and 19.39%, respectively. These results support the hypothesis that under drought stress, varieties with lower root metabolic costs seem to possess the ability to develop extensive and deep root systems to fully utilize soil water resources without yield losses (Figure 9). A previous study exploring the utility of RCS in barley under nutrient-deficient conditions indicated that by reducing root respiration, RCS can promote root growth and soil resource acquisition in barley (Schneider et al., 2017b). This is because some metabolic activities may diminish or stagnate as cells senesce, and senescent cells require less energy and nutrients, leading to reduced energy expenditure and metabolic costs (Postma and Lynch, 2011; Jaramillo et al., 2013; Hu et al., 2014b; Saengwilai et al., 2014).

Based on this, we speculate that whether in barley and cotton crops or under nutrient-deficient and drought-stress environments, the reduced metabolic consumption of photosynthetic products caused by RCS may not result from stress damage but rather an adaptive strategy. This complex mechanism helps plants to cope more effectively with environmental stresses while retaining energy for more important survival needs (Chimungu et al., 2014a; Chimungu et al., 2014a; Lynch et al., 2014; Saengwilai et al., 2014). Perhaps, in older root segments, RCS may reduce radial water transport when resources in the root edge have been depleted. Therefore, the loss of cortex means that the resource acquisition function of young root tissues changes to support function, axial transport, and storage of mature root tissue.

4.3 RCS mediates resource redistribution for root growth and improves drought tolerance

Under abiotic stress, resource redistribution during RCS is more important for increasing root absorption area and improving aboveground drought tolerance of plants than is reducing root respiration (Postma and Lynch, 2011; Jaramillo et al., 2013; Chimungu et al., 2014b) In addition, the enlargement of cortical cells and the reduction of cortical cell layers are important features of RCS. Research on corn has shown that under field water stress, varieties with large cortical cells had a root depth of 32% to 41%, a relative water content of 22% to 30% in the leaves, and a yield increase of 99% to 145% compared to varieties with small cortical cells (Chimungu et al., 2014b). Meanwhile, compared with varieties with increased cell layers in the root cortex, corn varieties with reduced cell layers in the root cortex had a root depth of 33% to 40%, a relative water content of 10% to 35% in the leaves, a biomass of 35% to 70% in the stems and leaves, and a yield increase of 33% to 114% (Chimungu et al., 2014a). This may be due to the release of a large amount of nutrients from aging cells in the cortex, which may significantly impact plant growth throughout the entire growth season by supporting higher growth rates and subsequent larger soil exploration (Lynch et al., 2014; Saengwilai et al., 2014). Therefore, in maize, growth was promoted under stress by increased cortical cell size and decreased number of root cortical cell layers. However, there are no reports on the impact of resource reallocation during RCS on the drought tolerance of cotton crops.

Based on the aboveground traits, this study is the first to explore the impact of resource redistribution during RCS on cotton drought tolerance. We found that RCS helps promote cotton growth, with "Guoxin 02" exhibiting greater root dry weight, total root length, specific root surface area, and convex hull area, as well as higher leaf water potential and relative leaf water content under drought stress. This is probably due to the changes in the root structure caused by the aging of the root cortex tissues, such as changes in internal cell walls and morphological adjustments. The correlation analysis indicated that RCS was significantly positively correlated with leaf water potential, leaf relative water content, and F v/F m ($p < 0.01$). These results support the hypothesis that RCS leads to more extensive branching and deeper roots, thereby expanding the surface area of the roots. This conferred the cotton plants with a stronger survival advantage by fully utilizing deep-water resources, enabling the plants to better adapt to arid environments and maintain normal aboveground growth while improving drought tolerance (Figure 9, Postma and Lynch, 2011; Schneider et

al., 2017a). We consider this effect as the self-catalytic effect.

4.4 IAA andABA regulate RCS

The intrinsic developmental signals of plants work in synergy with external environmental factors, inducing changes in different endogenous hormone levels within the plant, thereby regulating the aging process in plant tissues. Although some plant hormones, such as IAA and ABA, have been shown to regulate leaf senescence, their role in root senescence has not been fully elucidated (Schippers et al., 2015).

Our research found that the IAA content of "Guoxin 02" was significantly higher than that of "Ji 228", and its content increased with the increasing distance from the root tips (Figure 6C). This may be because IAA promotes cell elongation and volume increase, which increases the root growth to adapt to drought stress. Similar trends have also been reported in rice, indicating the key role of IAA in enhancing drought tolerance in rice seedlings (Zhang et al., 2009). Our study also found that increased IAA content could improve the drought tolerance of cotton, and the RCS degree of "Guoxin 02" is significantly increased with increased IAA content, indicating that IAA has a positive regulatory effect on plant RCS (Figures S1 D-F).

As a plant sesquiterpene, ABA is involved in regulating plant growth and development processes and responding to various biotic and abiotic stresses (Jibran et al., 2013). Our research showed that the ABA content decreased as the distance from the root tip increased (Figure 6E). This result is similar to that reported in barley, whereby the ABA content was higher in the root tip compared to the root basal zone (Liu et al., 2019). This is probably because the root tip is the growth point of the root system, with more active and complex cellular activities, promoting the activity of the ABA synthesis pathway. In addition, we found that the reduction of ABA could improve the drought tolerance of cotton and significantly increase the RCS degree of the drought-tolerance variety, suggesting the negative regulatory effect of ABA on cotton RCS (Figures S1 G-I).

In conclusion, this study confirms for the first time the presence of RCS in cotton, a dicotyledonous crop, and deeply explores the characteristics and patterns of RCS in cotton under drought stress. We systematically studied the characteristics, patterns, and interrelationships of root metabolic activity and endogenous hormones during the RCS, as well as their regulatory effects on roots and aboveground parts. We found that RCS enhances cotton drought tolerance by reducing root metabolic costs and regulating endogenous hormone content (Figure 10).

ACKNOWLEDGEMENT

This research was funded by National Natural Science Foundation of China (No. 32172120 and No.32272220).

CONFLICT OF INTEREST STATEMENT

The authors declare no conflict of interest.

DATA AVAILABILITY STATEMEN The data that has been used is confidential.

References

Antonietta Ciardiello M, Camardella L, Di Prisco G (1995) Glucose-6-phosphate dehydrogenase from the blood cells of two Antarctic teleosts: Correlation with cold adaptation. Biochimica et Biophysica Acta (BBA) - Protein Structure and Molecular Enzymology 1250: 76–82

Baldwin J, Elias JP, Wells RMG, Donovan DA (2007) Energy metabolism in the tropical abalone, Haliotis asinina Linné: Comparisons with temperate abalone species. Journal of Experimental Marine Biology and Ecology 342: 213–225

Beckel DKB (1956) Cortical disintegration in the roots of bouteloua gracilis (H.B.K) lag. New Phytologist 55: 183–190

Bingham IJ (2007) Quantifying the presence and absence of turgor for the spatial characterization of cortical senescence in roots of Triticum aestivum (Poaceae). American Journal of Botany 94: 2054–2058

Brown ME, Hornby D (1987) Effects of nitrate and ammonium on wheat roots in gnotobiotic culture: Amino acids, cortical cell death and take-all (caused by Gaeumannomyces graminis var. Tritici). Soil Biology and Biochemistry 19: 567–573

Childress JJ, Somero GN (1979) Depth-related enzymic activities in muscle, brain and heart of deep-living pelagic marine teleosts. Marine Biology 52: 273–283

Chimungu JG, Brown KM, Lynch JP (2014a) Reduced Root Cortical Cell File Number Improves Drought Tolerance in Maize. Plant Physiology 166: 1943–1955

Chimungu JG, Brown KM, Lynch JP (2014b) Large Root Cortical Cell Size Improves Drought Tolerance in Maize. Plant Physiology 166: 2166–2178

Chimungu JG, Maliro MFA, Nalivata PC, Kanyama-Phiri G, Brown KM, Lynch JP (2015) Utility of root cortical aerenchyma under water limited conditions in tropical maize (*Zea mays* L.). Field Crops Research 171: 86–98

Christopher J, Christopher M, Jennings R, Jones S, Fletcher S, Borrell A, Manschadi AM, Jordan D, Mace E, Hammer G (2013) QTL for root angle and number in a population developed from bread wheats (*Triticum aestivum*) with contrasting adaptation to water-limited environments. Theoretical and Applied Genetics 126: 1563–1574

Deacon JW, Henry CM (1978) Death of the cereal root cortex: its relevance to biological control of take-all. Annals of Applied Biology 89: 100–100

Deacon JW, Henry CM (1980) Age of wheat and barley roots and infection by gaeumannomyces graminis var tritici. Soil Biology and Biochemistry 12: 113–118

Deacon JW, Mitchell RT (1985) Comparison of rates of natural senescence of the root cortex of wheat (with and without mildew infection), barley, oats and rye. Plant and Soil 84: 129–131

Galindo-Castañeda T, Brown KM, Lynch JP (2018) Reduced root cortical burden improves growth and grain yield under low phosphorus availability in maize: Root cortical burden and phosphorus capture. Plant, Cell & Environment 41: 1579–1592

Gunawardena AHLAN, Pearce DM, Jackson MB, Hawes CR, Evans DE (2001) Characterisation of programmed cell death during aerenchyma formation induced by ethylene or hypoxia in roots of maize(*Zea mays* L.). Planta 212: 205–214

Guo C, Liu L, Sun H, Wang N, Zhang K, Zhang Y, Zhu J, Li A, Bai Z, Liu X, et al (2022) Predicting Fv/Fm and evaluating cotton drought tolerance using hyperspectral and 1D-CNN. Frontiers in Plant Science 13: 1007150

Henry CM, Deacon JW (1981) Natural (non-pathogenic) death of the cortex of wheat and barley seminal roots, as evidenced by nuclear staining with acridine orange. Plant and Soil 60: 255–274

Holden J (1975) Use of nuclear staining to assess rates of cell death in cortices of cereal roots. Soil Biology and Biochemistry 7: 333–334

Holden J (1976) Infection of wheat seminal roots by varieties of Phialophora radicicola and Gaeumannomyces graminis. Soil Biology and Biochemistry 8: 109–119

Hu B, Henry A, Brown KM, Lynch JP (2014a) Aerenchyma formed under phosphorus deficiency contributes to the reduced root hydraulic conductivity in maize. Annals of Botany 113: 181–189

Hu B, Henry A, Brown KM, Lynch JP (2014b) Root cortical aerenchyma inhibits radial nutrient transport in maize (*Zea mays*). Annals of Botany 113: 181–189

Jaramillo RE, Nord EA, Chimungu JG, Brown KM, Lynch JP (2013) Root cortical burden influences drought tolerance in maize. Annals of Botany 112: 429–437

Jibran R, A. Hunter D, P. Dijkwel P (2013) Hormonal regulation of leaf senescence through integration of developmental and stress signals. Plant Molecular Biology 82: 547–561

Jupp AP, Newman EI (1987) Morphology and anatomical Effects of severe drought on the roots of *Lolium perenne* L. The New Phytologist 105: 393–402

Lambers H (1979) Efficiency of Root Respiration in Relation to Growth Rate, Morphology and Soil Composition. Physiologia Plantarum 46: 194–202

Lewis SJ, Deacon JW (1982) Effects of shading and powdery mildew infection on senescence of the root cortex and coleoptile of wheat and barley seedlings, and implications for root- and foot-rot fungi. Plant and Soil 69: 401–411

Liljeroth E (1995) Comparisons of early root cortical senescence between barley cultivars, *Triticum* species and other cereals. New Phytologist 130: 495–501

Liljeroth E, Bryngelsson T (2001) DNA fragmentation in cereal roots indicative of programmed root cortical cell death. Physiologia Plantarum 111: 365–372

Liu Z, Marella CBN, Hartmann A, Hajirezaei MR, Von Wirén N (2019) An Age-Dependent Sequence of Physiological Processes Defines Developmental Root Senescence. Plant Physiol 181: 993–1007

Lynch JP (2015) Root phenes that reduce the metabolic costs of soil exploration: opportunities for 21st century agriculture: New roots for agriculture. Plant, Cell & Environment 38: 1775–1784

Lynch JP (2007) Roots of the Second Green Revolution. Australian Journal of Botany 55: 493

Lynch JP, Brown KM (2008) Root strategies for phosphorus acquisition. Plant Ecophysiology 7: 83–116

Lynch JP, Chimungu JG, Brown KM (2014) Root anatomical phenes associated with water acquisition from drying soil: targets for crop improvement. Journal of Experimental Botany 65: 6155–6166

Lynch JP, Ho MD, Phosphorus L (2005) Rhizoeconomics: Carbon costs of phosphorus acquisition. Plant and Soil 269: 45–56

Postma JA, Lynch JP (2011) Root Cortical Aerenchyma Enhances the Growth of Maize on Soils with Suboptimal Availability of Nitrogen, Phosphorus, and Potassium. Plant Physiology 156: 1190–1201

Pound MP, French AP, Atkinson JA, Wells DM, Bennett MJ, Pridmore T (2013) RootNav: Navigating Images of Complex Root Architectures. Plant Physiology 162: 1802–1814

Saengwilai P, Nord EA, Chimungu JG, Brown KM, Lynch JP (2014) Root Cortical Aerenchyma Enhances Nitrogen Acquisition from Low-Nitrogen Soils in Maize. Plant Physiology 166: 726–735

Schippers JHM, Schmidt R, Wagstaff C, Jing H-C (2015) Living to Die and Dying to Live: The Survival Strategy behind Leaf Senescence. Plant Physiology 169: 914–930

Schneider HM, Lynch JP (2018) Functional implications of root cortical senescence for soil resource capture. Plant and Soil 423: 13–26

Schneider HM, Postma JA, Wojciechowski T, Kuppe C, Lynch JP (2017a) Root Cortical Senescence Improves Growth under Suboptimal Availability of N, P, and K. Plant Physiol 174: 2333–2347

Schneider HM, Wojciechowski T, Postma JA, Brown KM, Lücke A, Zeisler V, Schreiber L, Lynch JP (2017b) Root cortical senescence decreases root respiration, nutrient content and radial water and nutrient transport in barley: Cortical senescence reduces respiration, nutrient content and radial transport. Plant, Cell & Environment 40: 1392–1408

Schneider HM, Wojciechowski T, Postma JA, Brown KM, Lynch JP (2018) Ethylene modulates root cortical senescence in barley. Annals of Botany 122: 95–105

Schussler EE, Longstreth DJ (1996) Aerenchyma develops by cell lysis in roots and cell separation in leaf petioles in *Sagittaria lancifolia* (Alismataceae). American Journal of Botany 83: 1266–1273

Sun L, Ataka M, Han M, Han Y, Gan D, Xu T, Guo Y, Zhu B (2021) Root exudation as a major competitive fine-root functional trait of 18 coexisting species in a subtropical forest. The New Phytologist 229: 259–271

Van Der Werf A, Kooijman A, Welschen R, Lambers H (1988) Respiratory energy costs for the maintenance of biomass, for growth and for ion uptake in roots of *Carex diandra* and *Carex acutiformis* . Physiologia Plantarum 72: 483–491

Wenzel CL, McCully ME (1991) Early senescence of cortical cells in the roots of cereals. How good is the evidence? American Journal of Botany 78: 1528–1541

Yang Z, Tian J, Wang Z, Feng K (2022) Monitoring the photosynthetic performance of grape leaves using a hyperspectral-based machine learning model. European Journal of Agronomy 140: 126589

Yeates JS, Parker CA (1986) Rate of natural senescence of seminal root cortical cells of wheat, barley and oats, with reference to invasion by Gaeumannomyces graminis. Transactions of the British Mycological Society 86: 683–685

Zhang G, Chen M, Li L, Xu Z, Chen X, Guo J, Ma Y (2009) Overexpression of the soybean GmERF3 gene, an AP2/ERF type transcription factor for increased tolerances to salt, drought, and diseases in transgenic tobacco. Journal of Experimental Botany 60: 3781–3796

Zhang Y, Zhong Y, Gao C, Dong Z, Chen N, Wang M (2013) Determination of five endogenous hormones in wheat by high performance liquid chromatography. Chinese Journal of Chromatography 31: 800

Zhang Z, Zhu L, Li D, Wang N, Sun H, Zhang Y, Zhang K, Li A, Bai Z, Li C, et al (2021) In situ Root Phenotypes of Cotton Seedlings Under Phosphorus Stress Revealed Through RhizoPot. Frontiers in Plant Science 12: 716691

Figure legends

FIGURE 1 The transverse cross-sections of the taproot of "Guoxin 02" and "Ji 228" varieties sampled at different areas on the taproot 15 days after the treatment and stained with acridine orange fluorescent nuclei. Note: acridine orange fluorescent nuclei are not visible in these images because they are located deeper within the tissue, as indicated by a laser scanning confocal microscope. The red arrow indicates the lacunae area.

FIGURE 2 Characteristics and occurrence mechanisms of RCS in different cotton varieties after 15 days of drought stress. Statistical analysis of (A) the cortical senescence percentage, (B) cortical cell files and (C) the cortical lacunae area. DT type, Drought-tolerant type "Guoxin 02"; DS type, Drought-sensitive type "Ji 228"; NS, no-stress; DS, drought stress; C, varieties; D, drought. Error bars represent standard errors of the means. Different lowercase letters in the figure indicate significant differences between the same root segments from different cotton varieties under drought stress treatments (p [?] 0.05). P ¿0.05, no significance (ns);P ¡0.01 significant difference (**).

FIGURE 3 Effects of the drought treatment on the root metabolic costs of cotton. Statistical analysis of (A) phosphofructokinase, (B) malate dehydrogenase, (C) glucose-6-phosphate dehydrogenase, and (D) root respiration activities at 3 cm, 6 cm, 9 cm, and 12 cm segments from the taproot tips of the "Guoxin 02" and "Ji 228". (E) Comparative image showing the differences in root metabolic costs between "Guoxin 02" and "Ji 228" under drought stress. Long and short arrows represent higher and lower metabolic costs, respectively. DT type, Drought-tolerant type "Guoxin 02"; DS type, Drought-sensitive type "Ji 228"; NS, no-stress; DS, drought stress; C, varieties; D, drought. Error bars represent standard errors of the means. P ¿0.05, P ¡0.05 and$P$ ¡0.01 indicate no significance (ns), significant difference (*) and highly significant difference (**), respectively. Different lowercase letters in the figure indicate significant differences between different root segments under the same treatment (P [?] 0.05).

FIGURE 4 Linear regression analysis showing the relationship between RCS and root growth, root metabolic costs, and aboveground growth under drought stress. (A) Total root length, (B) root dry weight, (C) root tissue density, (D) root respiration at 6 cm from the root tip, (E) root respiration at 9 cm from the root tip, (F) root respiration at 12 cm from the root tip, (G) leaf water potential, (H) leaf relative water content, and (I) the ratio of variable to maximum fluorescence (F v/F m).

FIGURE 5 Effects of drought stress on the ratio and size of root cross-section in the two cotton varieties. (A) Representative image of the root tissue size of "Guoxin 02" under drought stress. Statistical analysis of (B) stele/whole ratio, (C) cortex/stele ratio, and (D) lacunae/cortex ratio at the 3 cm, 6 cm, 9 cm, and 12 segments cm from the root tips of "Guoxin 02" and "Ji 228". NS, no-stress; DS, drought stress; C, varieties; D, drought. Error bars represent standard errors of the means. P ¿0.05, no significance (ns); P ¡0.01 significant difference (**). Different lowercase letters in the figure indicate significant differences between different root segments under the same treatment (P [?] 0.05).

FIGURE 6 Effects of the drought treatment on phytohormone levels in the two cotton varieties. Statistical analysis of (A) gibberellin, (B) zeatin riboside, (C) indole-3-acetic acid, (D) brassinolide, and (E) abscisic acid contents at the 3 cm, 6 cm, 9 cm, and 12 cm segments from the taproot tips of the "Guoxin 02" and "Ji 228". DT type, Drought-tolerant type "Guoxin 02"; DS type, Drought-sensitive type "Ji 228"; NS, no-stress; DS, drought stress. Error bars represent standard errors of the means. P ¿0.05, no significance (ns); P ¡0.05, significant difference (*);P ¡0.01, highly significant difference (**). Different lowercase letters in the figure indicate significant differences between different root segments under the same treatment (P [?] 0.05).

FIGURE 7 Effects of drought stress on the root traits of "Guoxin 02" and "Ji 228". (A) Representative images of root traits of the two varieties at 5 d, 10 d and 15 d after drought stress. Statistical analysis of the (B) total root length, (C) root dry weight, (D) specific root surface area, (E) root volume, (F) average diameter, (G) root tissue density, (H) taproot length, (I) average length-lateral roots, (J) Average length-all root, (K) lateral root angle, (L) lateral root count, and (M) convex hull area. DT type, Drought-tolerant type "Guoxin 02"; DS type, Drought-sensitive type "Ji 228". NS, no-stress; DS, drought stress; C, varieties; D, drought. Error bars represent standard errors of the means. P ¡0.05, significant difference (*); P ¡0.01, highly significant difference (**).

FIGURE 8 Effects of drought stress on the aboveground traits of "Guoxin 02" and "Ji 228". (A) Representative images of the growth of "Guoxin 02" and "Ji 228" at 0, 5, 10 and 15 days after drought stress. Statistical analysis of the (B) ratio of variable to maximum fluorescence (F v/F m), (C) leaf area, (D) leaf water potential, (E) steam diameter, (F) leaf water saturation deficit, (G) plant height, (H) relative water content, (I) SPAD value, (J) stomatal length, (K) stomatal width, (L) stomatal opening, and (M) stomatal density. DT type, drought-tolerant type "Guoxin 02"; DS type, drought-sensitive type "Ji 228". CK, no-stress; DS, drought stress; C, varieties; D, drought. Error bars represent standard errors of the means. P ¿0.05, no significance (ns); P ¡0.01, highly significant difference (**). Different lowercase letters in the figure indicate significant differences among different varieties and treatments at the same time point (P [?] 0.05).

FIGURE 9 Structural equation modeling showing the effect of RCS on drought tolerance of cotton under drought stress. The standardized loading coefficients are indicated by the numbers. Positive loading coefficients signify positive correlations between the measured variables and the factors, while negative loading coefficients indicate negative correlations. The red solid and dashed lines represent positive and negative correlations, respectively.

FIGURE 10 The regulatory model and function of RCS in the root growth and development of different cotton varieties. Comparative analysis of the regulatory mechanism of RCS on drought tolerance of the different cotton under drought stress. In drought-tolerance varieties, endogenous hormones (showing increased indole-3-acetic acid and reduced abscisic acid contents) are involved in the regulation of RCS. Increased lacunae/cortex ratio, reduced cortical cell files and cortex/stele ratio, further reduced root respiration and metabolic enzyme activity (phosphofructokinase, malate dehydrogenase and glucose-6-phosphate dehydrogenase). This might be due to the redistribution of more resources to root growth (reflected by increased

root dry weight, total root length, and convex hull area), ultimately increasing the aboveground drought tolerance (reflected by increased leaf water potential, relative leaf water content, and stomatal opening under drought stress). The regulatory mechanism of RCS varies based on plant species, drought severity and specific growth stages. "Ji 228" exhibited a lower incidence of RCS than "Guoxin 02". Pink arrows denote positive regulation, while green arrows indicate negative regulation. Long and short arrows represent higher and lower metabolic costs, respectively.

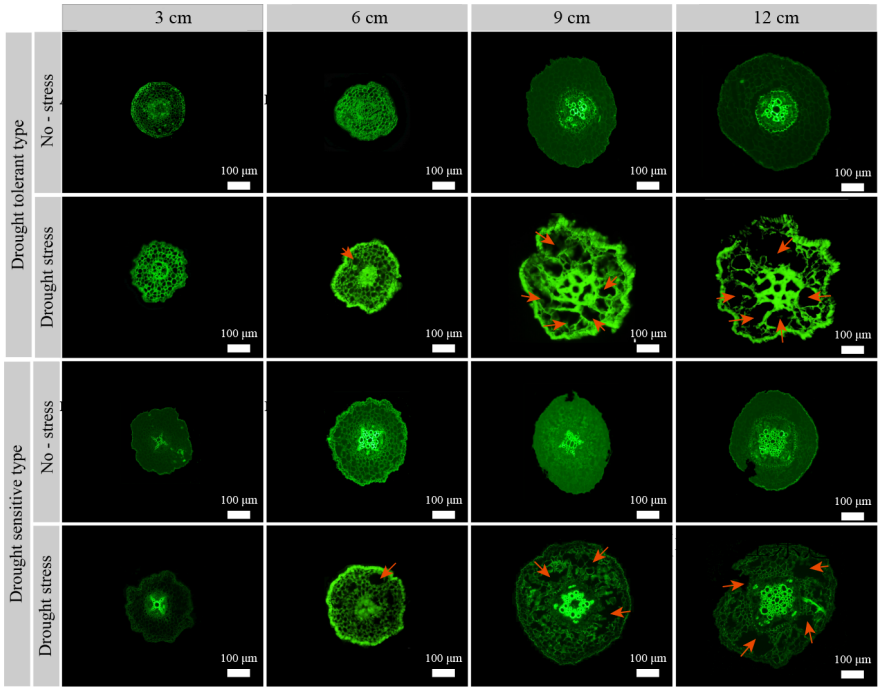

FIGURE 1 The transverse cross-sections of the taproot of "Guoxin 02" and "Ji 228" varieties sampled at different areas on the taproot 15 days after the treatment and stained with acridine orange fluorescent nuclei. Note: acridine orange fluorescent nuclei are not visible in these images because they are located deeper within the tissue, as indicated by a laser scanning confocal microscope. The red arrow indicates the lacunae area.

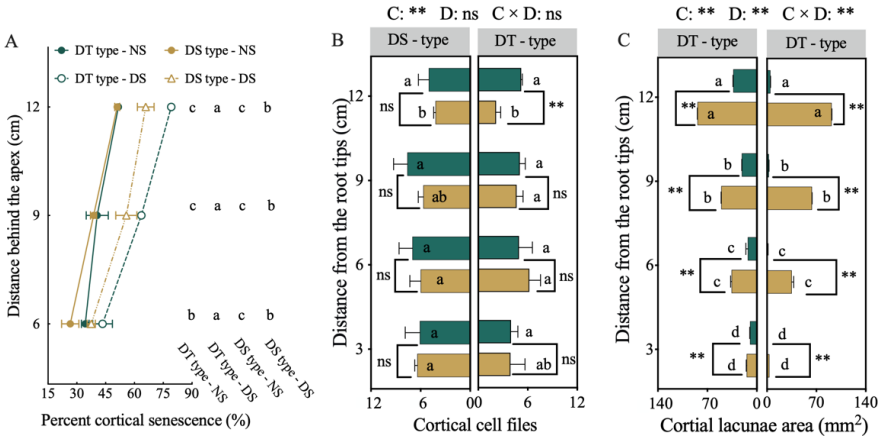

FIGURE 2 Characteristics and occurrence mechanisms of RCS in different cotton varieties after 15 days of

drought stress. Statistical analysis of (A) the cortical senescence percentage, (B) cortical cell files and (C) the cortical lacunae area. DT type, Drought-tolerant type "Guoxin 02"; DS type, Drought-sensitive type "Ji 228"; NS, no-stress; DS, drought stress; C, varieties; D, drought. Error bars represent standard errors of the means. Different lowercase letters in the figure indicate significant differences between the same root segments from different cotton varieties under drought stress treatments (p [?] 0.05).P ¿0.05, no significance (ns); P ¡0.01 significant difference (**).

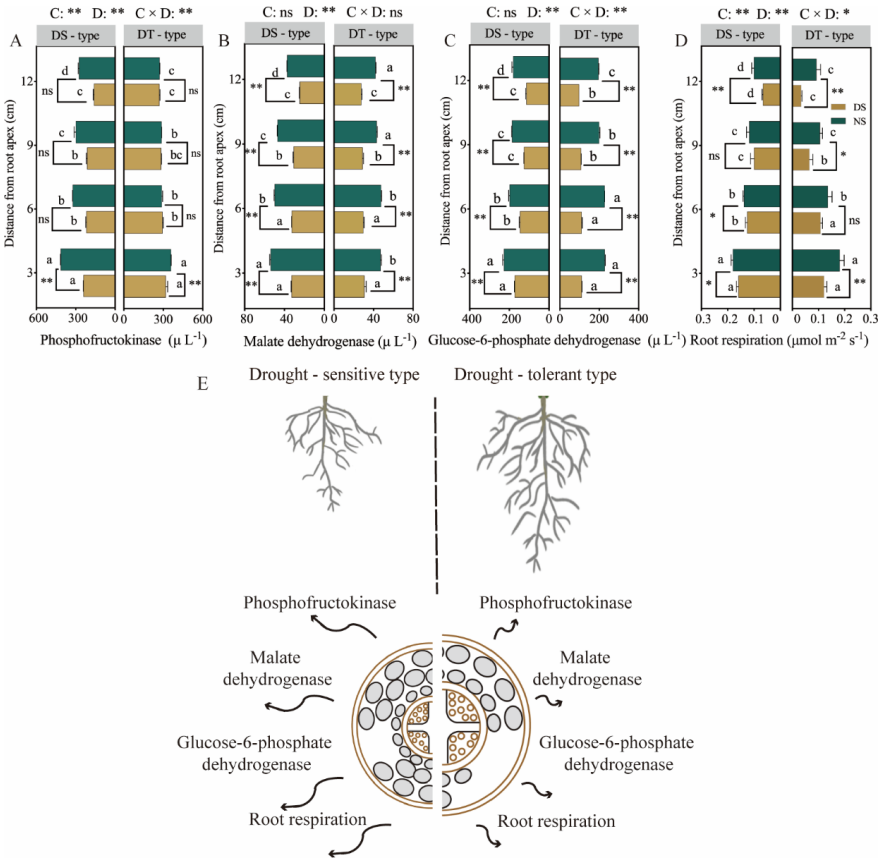

FIGURE 3 Effects of the drought treatment on the root metabolic costs of cotton. Statistical analysis of (A) phosphofructokinase, (B) malate dehydrogenase, (C) glucose-6-phosphate dehydrogenase, and (D) root respiration activities at 3 cm, 6 cm, 9 cm, and 12 cm segments from the taproot tips of the "Guoxin 02" and "Ji 228". DT type, Drought-tolerant type "Guoxin 02"; DS type, Drought-sensitive type "Ji 228"; NS, no-stress; DS, drought stress; C, varieties; D, drought. Error bars represent standard errors of the means. P ¿0.05,P ¡0.05 and P ¡0.01 indicate no significance (ns), significant difference (*) and highly significant difference (**), respectively. Different lowercase letters in the figure indicate significant differences between different root segments under the same treatment (P [?] 0.05).

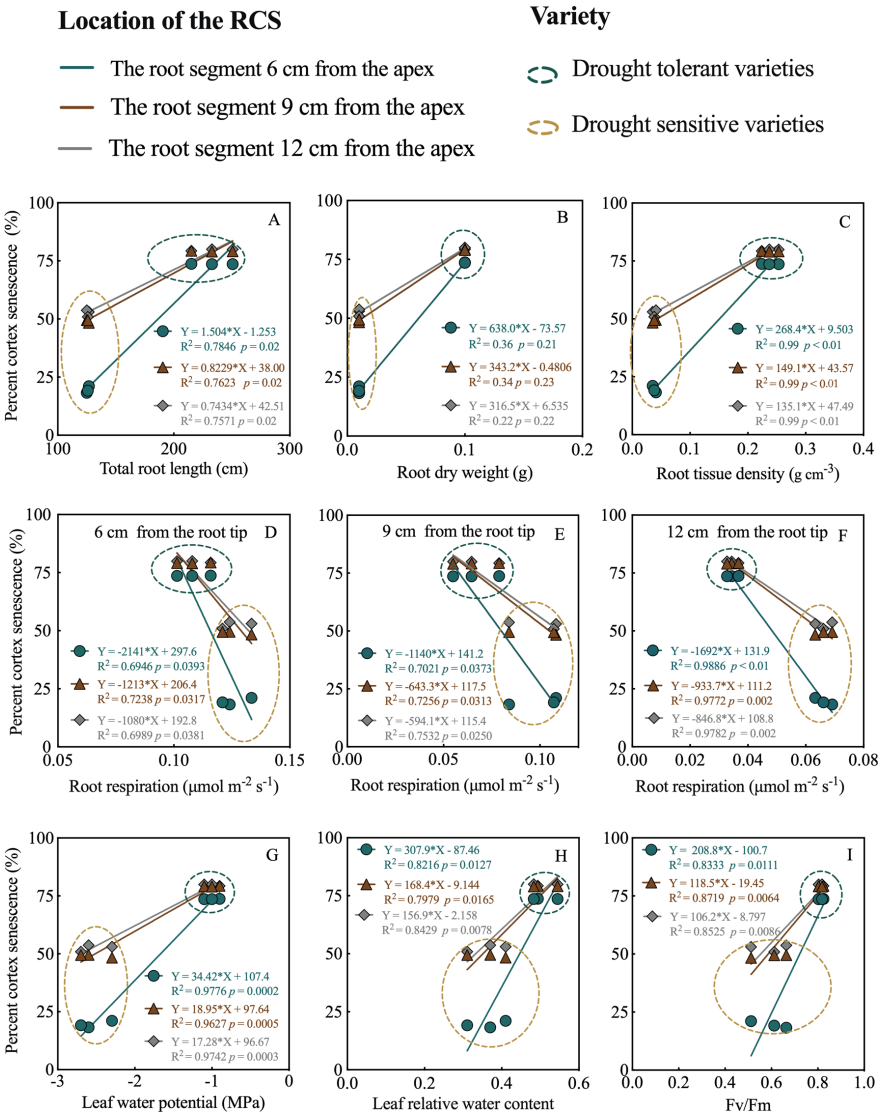

FIGURE 4 Linear regression analysis showing the relationship between RCS and root growth, root metabolic costs, and aboveground growth under drought stress. (A) Total root length, (B) root dry weight, (C) root tissue density, (D) root respiration at 6 cm from the root tip, (E) root respiration at 9 cm from the root tip, (F) root respiration at 12 cm from the root tip, (G) leaf water potential, (H) leaf relative water content, and (I) the ratio of variable to maximum fluorescence (F v/F m).

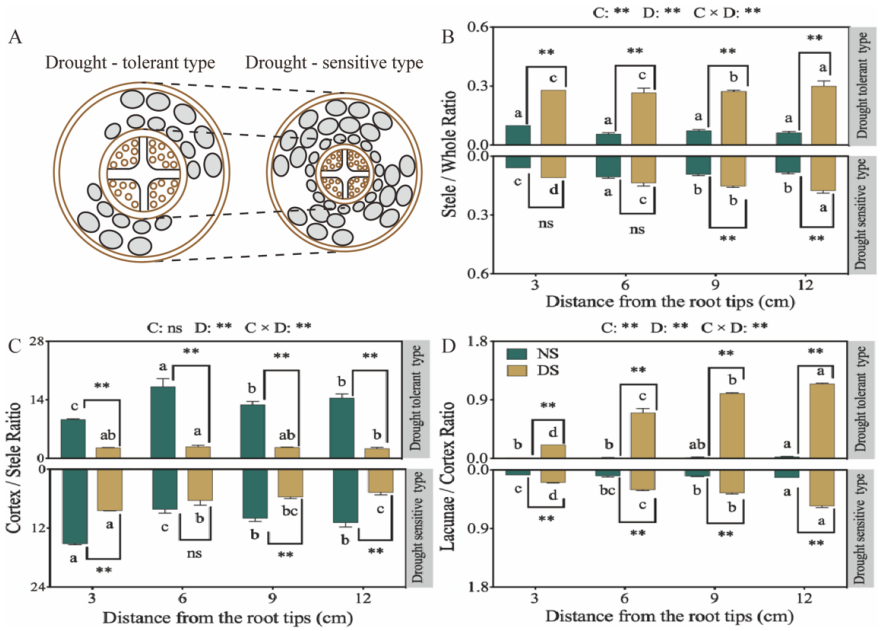

FIGURE 5 Effects of drought stress on the ratio and size of root cross-section in the two cotton varieties. (A) Representative image of the root tissue size of "Guoxin 02" under drought stress. Statistical analysis of (B) stele/whole ratio, (C) cortex/stele ratio, and (D) lacunae/cortex ratio at the 3 cm, 6 cm, 9 cm, and 12 segments cm from the root tips of "Guoxin 02" and "Ji 228". NS, no-stress; DS, drought stress; C, varieties; D, drought. Error bars represent standard errors of the means. P ¿0.05, no significance (ns); P ¡0.01 significant difference (**). Different lowercase letters in the figure indicate significant differences between different root segments under the same treatment (P [?] 0.05)

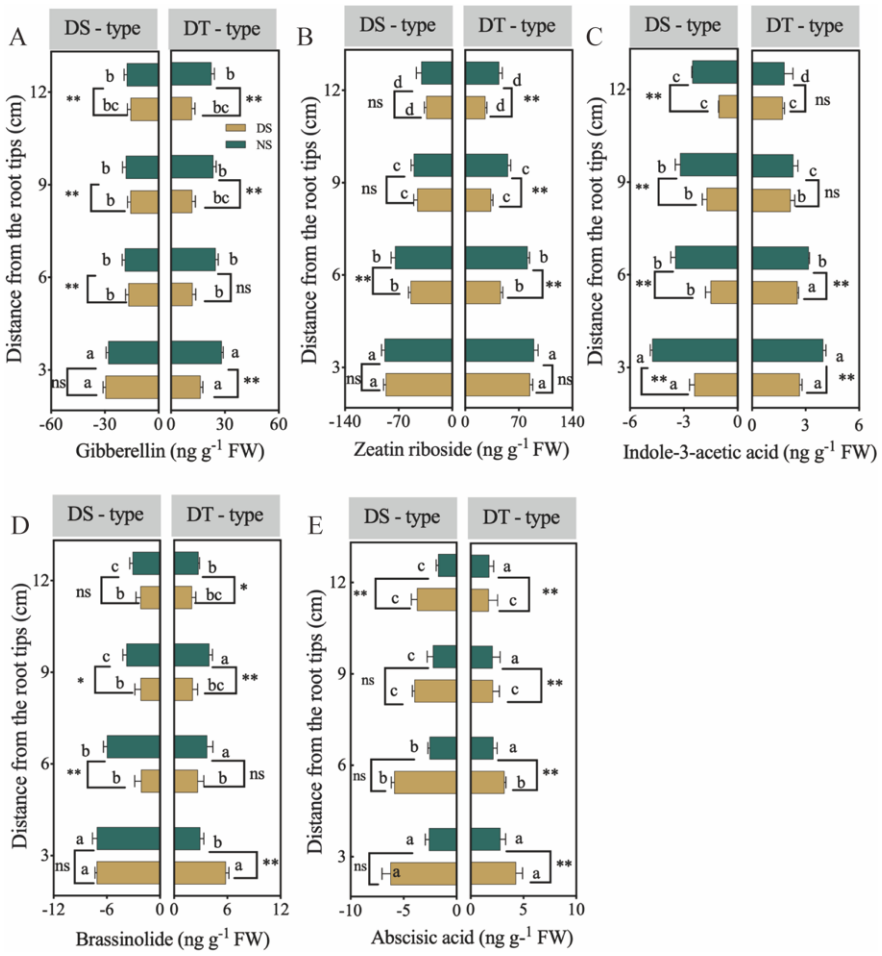

FIGURE 6 Effects of the drought treatment on phytohormone levels in the two cotton varieties. Statistical analysis of (A) gibberellin, (B) zeatin riboside, (C) indole-3-acetic acid, (D) brassinolide, and (E) abscisic acid contents at the 3 cm, 6 cm, 9 cm, and 12 cm segments from the taproot tips of the "Guoxin 02" and "Ji 228". DT type, Drought-tolerant type "Guoxin 02"; DS type, Drought-sensitive type "Ji 228"; NS, no-stress; DS, drought stress. Error bars represent standard errors of the means. P ¿0.05, no significance (ns); P ¡0.05, significant difference (*);P ¡0.01, highly significant difference (**). Different lowercase letters in the figure indicate significant differences between different root segments under the same treatment (P [?] 0.05).

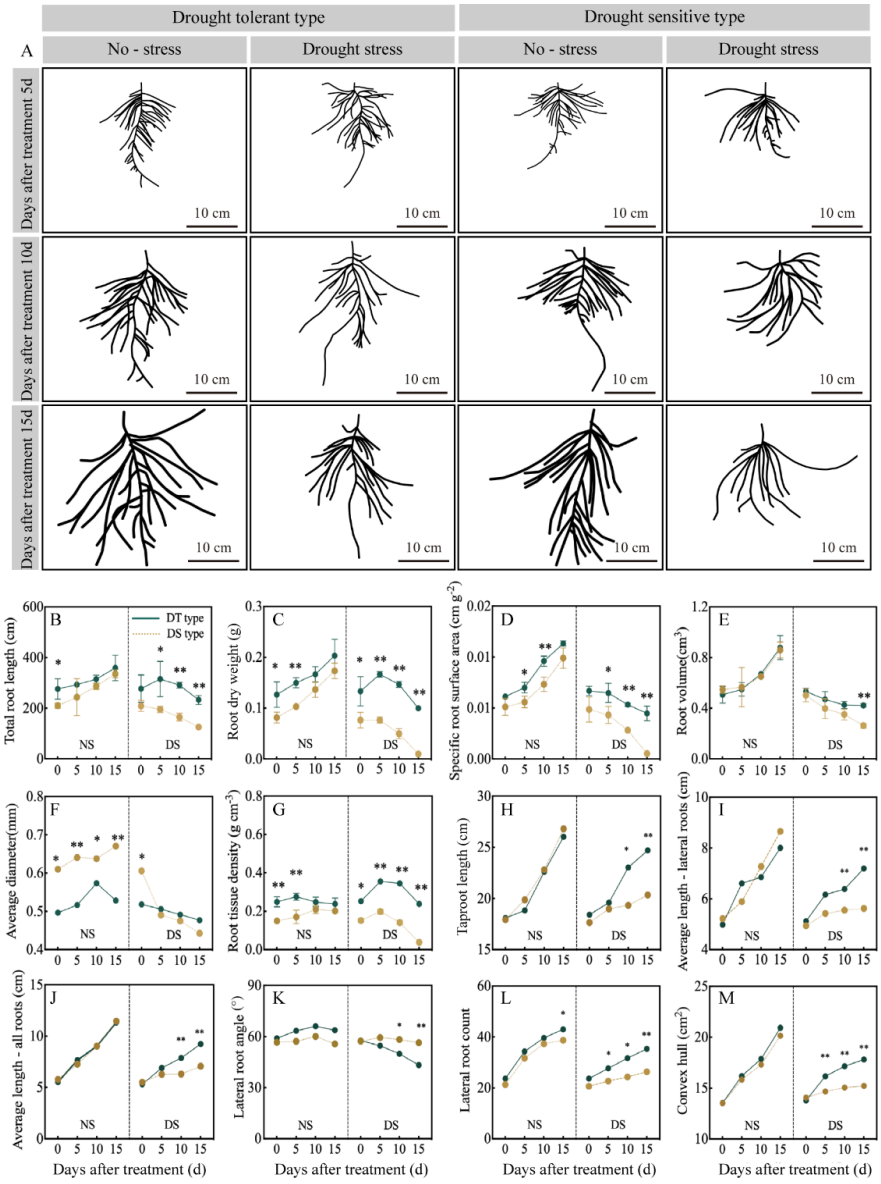

FIGURE 7 Effects of drought stress on the root traits of "Guoxin 02" and "Ji 228". (A) Representative images of root traits of the two varieties at 5d, 10d and 15d after drought stress. Statistical analysis of the (B) total root length, (C) root dry weight, (D) specific root surface area, (E) root volume, (F) average diameter, (G) root tissue density, (H) taproot length, (I) average length-lateral roots, (J) Average length-all root, (K) lateral root angle, (L) lateral root count, and (M) convex hull area. DT type, Drought-tolerant type "Guoxin 02"; DS type, Drought-sensitive type "Ji 228". NS, no-stress; DS, drought stress; C, varieties; D, drought. Error bars represent standard errors of the means. P ¡0.05, significant difference (*);P ¡0.01, highly significant difference (**).

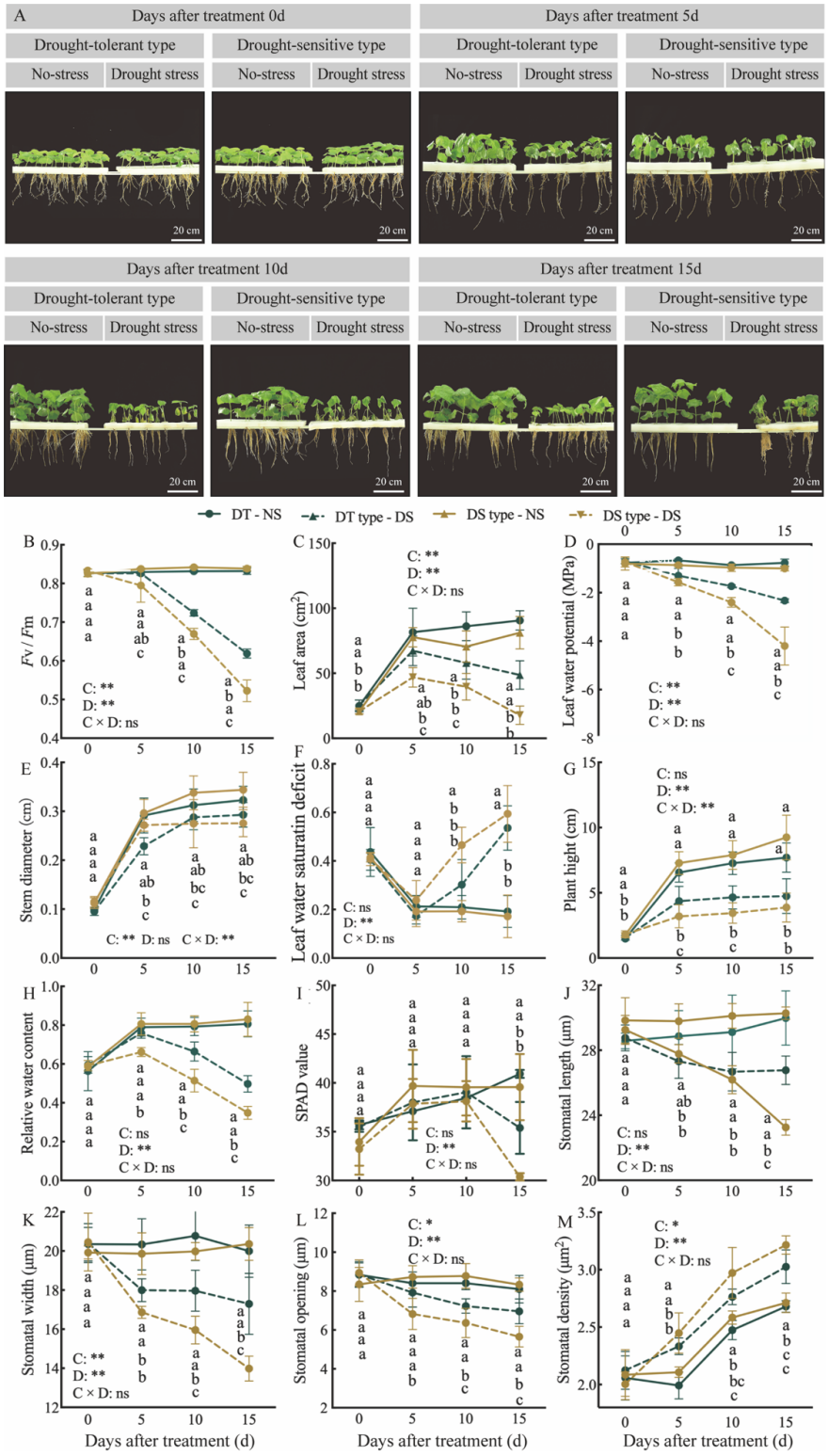

FIGURE 8 Effects of drought stress on the aboveground traits of "Guoxin 02" and "Ji 228". (A) Representative images of the growth of "Guoxin 02" and "Ji 228" at 0d, 5d, 10d, and 15d after drought stress.

Statistical analysis of the (B) ratio of variable to maximum fluorescence (F v/F m), (C) leaf area, (D) leaf water potential, (E) steam diameter, (F) leaf water saturation deficit, (G) plant height, (H) relative water content, (I) SPAD value, (J) stomatal length, (K) stomatal width, (L) stomatal opening, and (M) stomatal density. DT type, drought-tolerant type "Guoxin 02"; DS type, drought-sensitive type "Ji 228". CK, no-stress; DS, drought stress; C, varieties; D, drought. Error bars represent standard errors of the means. P ¿0.05, no significance (ns); P ¡0.01, highly significant difference (**). Different lowercase letters in the figure indicate significant differences among different varieties and treatments at the same time point (P [?] 0.05).

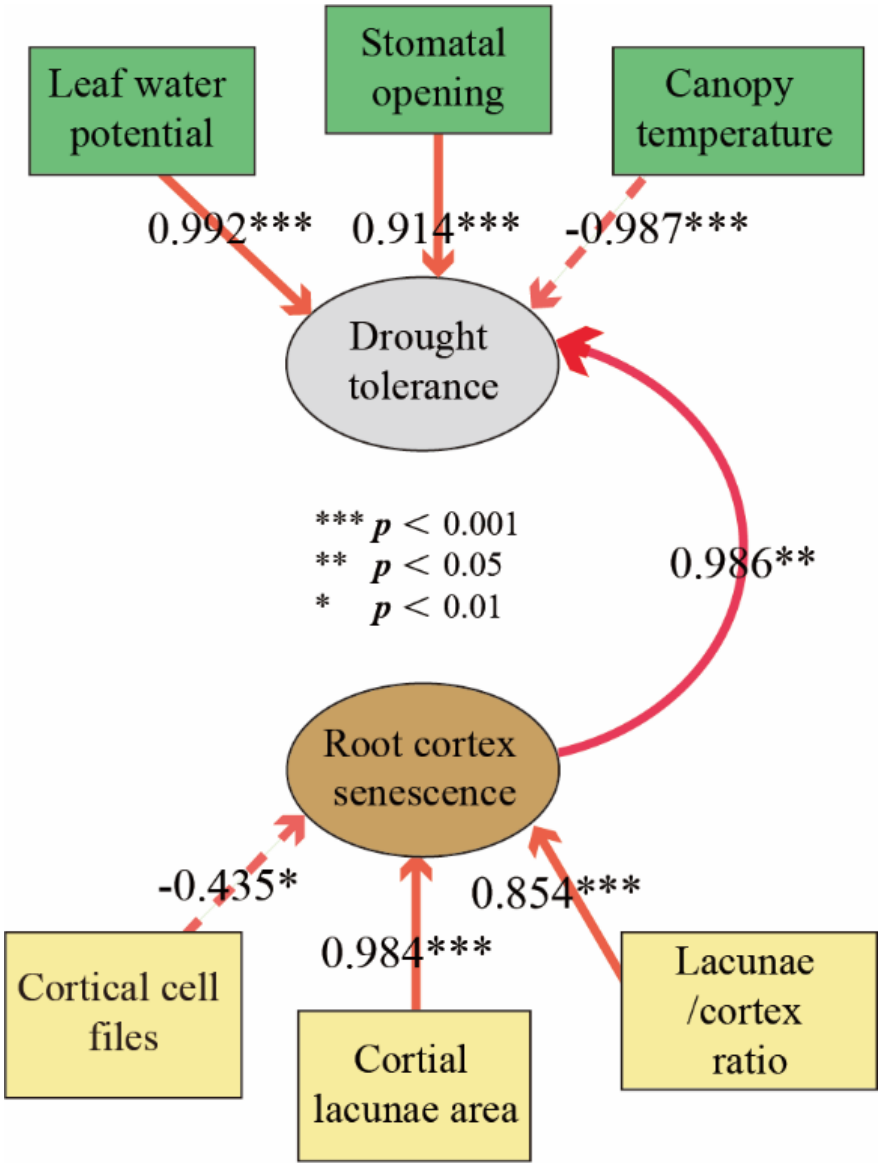

FIGURE 9 Structural equation modeling showing the effect of root cortical senescence (RCS) on drought tolerance of cotton under drought stress. The standardized loading coefficients are indicated by the numbers. Positive loading coefficients signify positive correlations between the measured variables and the factors, while negative loading coefficients indicate negative correlations. The red solid and dashed lines represent positive and negative correlations, respectively.

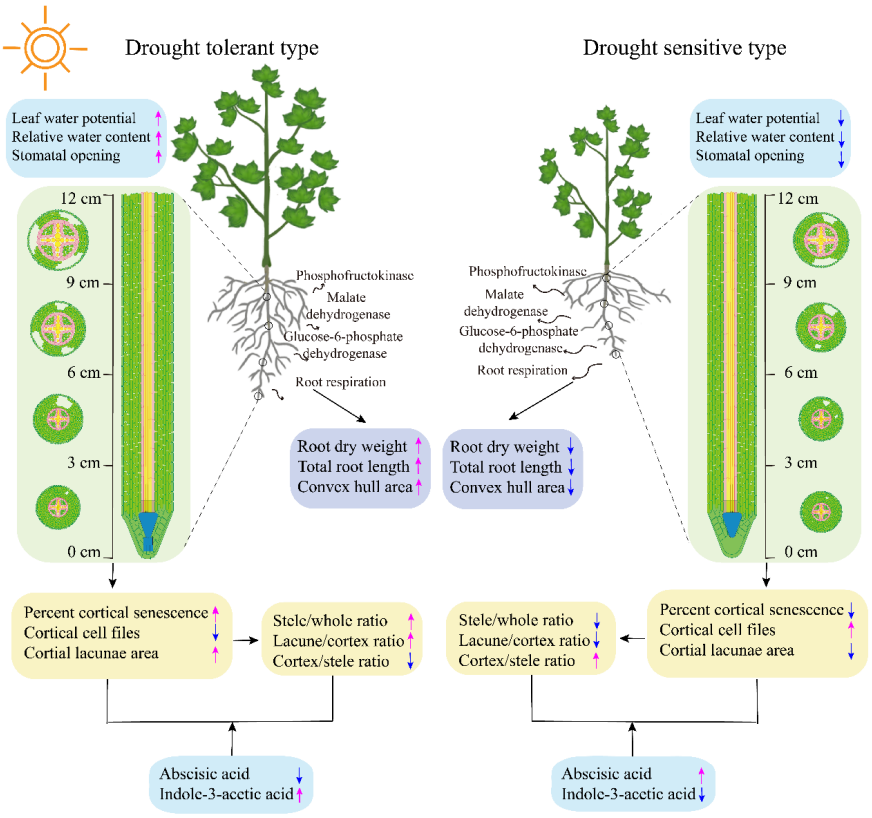

FIGURE 10 The regulatory model and function of root cortical senescence (RCS) in the root growth and development of different cotton varieties. Comparative analysis of the regulatory mechanism of RCS on drought tolerance of the different cotton under drought stress. In drought-tolerance varieties, endogenous hormones (showing increased indole-3-acetic acid and reduced abscisic acid contents) are involved in the regulation of RCS. Increased lacunae/cortex ratio, reduced cortical cell files and cortex/stele ratio, further reduced root respiration and metabolic enzyme activity (phosphofructokinase, malate dehydrogenase and glucose-6-phosphate dehydrogenase). This might be due to the redistribution of more resources to root growth (reflected by increased root dry weight, total root length, and convex hull area), ultimately increasing the aboveground drought tolerance (reflected by increased leaf water potential, relative leaf water content, and stomatal opening under drought stress). The regulatory mechanism of RCS varies based on plant species, drought severity and specific growth stages. "Ji 228" exhibited a lower incidence of RCS than "Guoxin 02". Pink arrows denote positive regulation, while green arrows indicate negative regulation. Long and short arrows represent higher and lower metabolic costs, respectively.